Assembly of Amphiphilic Phenylacetylene Macrocycles at the Air−Water Interface and on Solid Surfaces

Ashok S. Shetty, Pamela R. Fischer, Kurt F. Stork, Paul W. Bohn,* and Jeffrey S. Moore*

Contribution from the Departments of Chemistry, Materials Science and Engineering and The Beckman Institute for Advanced Science and Technology, University of Illinois, Urbana, Illinois 61801

Received May 9, 1996[⊗]

Abstract: The assembly of amphiphilic phenylacetylene macrocycles (PAMs), with molecular structures that vary in terms of the nature and orientation of their pendant functional groups, has been studied on a Langmuir−Blodgett trough and after transfer onto solid substrates. These monolayer films are of interest as two-dimensional host matrices and shape selective membranes whose two-dimensional organization should bring together shape selective compartments. The disk-like PAMs can, in principle, adopt orientations in which the plane of the macrocycle can range from perpendicular (edge-on) to parallel (face-on) at the interface. PAMs functionalized with six hydrophilic groups around the periphery do not prefer the face-on orientation and are most likely tilted, perhaps in a poorly organized state. PAMs that have spatially segregated hydrophilic and hydrophobic groups adopt the edge-on orientation when the hydrophilic moieties are carboxylate groups. In contrast, PAMs appended with acid moieties do not lead to stable monolayers, most likely because they engage in strong intermolecular hydrogen bonding interactions as evidenced by ^{1}H NMR and vapor pressure osmometry of the solutions. Monolayers of the dicarboxylate PAMs were transferred onto fused silica and Si(100) surfaces and these were in turn characterized by contact angle, ellipsometry, absorption FTIR, and angle-resolved X-ray photoelectron spectroscopies. Taken together these characterization experiments strongly support the hypothesis that the dicarboxylate PAMs form a well-ordered and stable two-dimensional array and that they adopt the edge-on configuration with near-vertical orientation of the macrocycle plane.

Introduction

The fabrication of monolayer films with interesting structural and material properties using Langmuir-Blodgett (LB) and self−assembled (SA) techniques is well documented.[1] Amphiphilic molecules used to construct organic thin films using the LB technique are predominantly rod-like molecules such as long-chain fatty acids and alcohols.[2] While these rod-like molecules more readily yield relatively robust monolayers, disk-shaped molecules with prefabricated cavities have a greater potential to form porous thin films or membranes which could effect interesting molecular separations or function as sensors.[3] Examples of disk-shaped molecules that have been shown to form stable LB films are porphyrins,[4] phthalocyanines,[5] triphenylene,[6] crown ethers,[7] and calixarenes.[3,8]

Here we describe the assembly of a novel class of disk-shaped molecules based on amphiphilic phenylacetylene macrocycles (PAMs) as monolayers, at the air−water interface and on the surfaces of solids. PAMs are a family of toroidal molecules with a geometrically well defined or "shape-persistent" macrocyclic skeleton and a cavity that spans approximately 8 Å in diameter. The synthetic strategy utilized for their construction has lead to PAMs that demonstrate cofacial aggregation in solution,[9] in discotic liquid crystalline phases[10] and in host crystalline solids.[11] This therefore paves the way for the design

* Authors to whom correspondence should be addressed.

[⊗] Abstract published in *Advance ACS Abstracts,* September 15, 1996.

(1) (a) Ulman, A. *An Introduction to Ultrathin Organic Films: From Langmuir−Blodgett to Self-Assembly*; Academic Press: Boston, 1991. (b) Roberts, G. G., Ed. *Langmuir−Blodgett Films*; Plenum Press: New York, 1990.

(2) Mingotaud, A-F.; Mingotaud, C.; Patterson, L. K. *Handbook of Monolayers*; Academic Press: San Diego, 1993; Vols. I and II.

(3) Markowitz, M. A.; Janout, V.; Castner, D. G.; Regen, S. L. *J. Am. Chem. Soc.* **1989**, *111*, 8192.

(4) (a) Bull, R. A.; Bulkowski, J. E. *J. Colloid Interface Sci*. **1983**, *92*, 1. (b) Hopf, F. R.; Möbius, D.; Whitten, D. G. *J. Am. Chem. Soc.* **1976**, *98*, 1584. (c) Vandevyer, M.; Barraud, A.; Ruaudel-Teixier, A.; Maillard, P.; Gianotti, C. *J. Colloid Interface Sci.* **1982**, *85*, 571. (d) Schmehl, R. H.; Shaw, G. L.; Whitten, D. G. *Chem. Phys. Lett.* **1978**, *58*, 549. (e) Adler, G. *J. Colloid Interface Sci.* **1979**, *72*, 164. (f) Jones, R.; Tredgold, R. H.; Hodge, P. *Thin Solid Films* **1983**, *99*, 25. (g) Ruaudel-Teixier, A.; Barraud, A.; Belbeoch, B.; Roulliay, M. *Thin Solid Films* **1983**, *99*, 33. (h) Vandevyer, M.; Barraud, A.; Ruaudel-Teixier, A. *Mol. Cryst. Liq. Cryst.* **1983**, *96*, 361. (i) Lecomte, C.; Baudin, C.; Ruaudel-Teixier, A.; Barraud, A.; Momenteau, M. *Thin Solid Films* **1985,** *133*, 103. (j) Luk, S.; Mayers, F. R.; Williams, J. O. *J. Chem. Soc., Chem. Commun.* **1987**, 215. (k) Schick, G. A.; Schreiman, I. C.; Wagner, R. W.; Lindsey, J. S.; Bocian, D. F. *J. Am. Chem. Soc.* **1989**, *111*, 1344.

(5) (a) Baker, S.; Petty, M. C.; Roberts, G. G.; Twigg, M. V. *Thin Solid Films* **1983,** *99*, 53. (b) Kovacs, G. J.; Loutfy, R. O.; Vincett, P. S.; Jenning, C.; Aroca, R. *Langmuir* **1986**, *2*, 689. (c) Fujiki, M.; Tabei, H. *Langmuir* **1988**, *4*, 320. (d) Ogawa, K.; Kinoshita, S.; Yonehara, H.; Nakahara, H.; Fukuda, K. *J. Chem. Soc., Chem. Commun.* **1989**, 477. (e) Palacin, S.; Barraud, A. *J. Chem. Soc., Chem. Commun*. **1989**, 45. (f) Ko, W. H.; Fu, C. W.; Wang, H. Y.; Batzel, D. A.; Kenney, M. E.; Lando, J. B. *Sens. Mater*. **1990**, *2*, 39. (g) Wang, H. Y.; Ko, W. H.; Batzel, D. A.; Kenney, M. E.; Lando, J. B. *Sens. Actuators* **1990**, *B1*, 138.

(6) (a) Albrecht, A.; Cumming, W.; Kreuder, A.; Laschewskyj, A.; Ringsdorf, H. *Colloid Polym. Sci*. **1986**, *264*, 659. (b) Orthmann, E.; Wegner, G. *Angew. Chem*. **1986**, *98*, 1114. (c) Karthaus, O.; Ringsdof, H.; Tsukruk, V. V.; Wendorff, J. H. *Langmuir* **1992**, *8*, 2279. (d) Josefowicz, J. Y.; Maliszewskyj, N. C.; Idziak, S. H. J.; Heiney, P. A.; McCauley, J. P.; Smith, A. B., III *Science* **1993**, *260*, 323. (e) Maliszewskyj, N. C.; Heiney, P. A.; Josefowicz, J. Y.; McCauley, J. P.; Smith, A. B., III *Science* **1994**, *264*, 77.

(7) (a) Dong, X.; Yang, X. M.; Zhu, Y. M.; Lu, Z. H.; Wei, Y. *Thin Solid Films* **1994**, *251*, 40. (b) Zhu, Y. M.; Jia, X. B.; Xiao, D.; Lu, Z. H.; Wei, Y.; Wu, Z. H.; Hu, Z. L.; Xie, M. *Phys. Lett. A* **1994**, *188*, 287. (c) Luboch, E.; Biernat, J. F.; Muszalska, E.; Bilewicz, R. *Supramol. Chem.* **1995**, *5*, 201. (d) Lednev, I. K.; Petty, M. C. *J. Phys. Chem.* **1995**, *99*, 4176.

(8) (a) Nakamoto, Y.; Kallinowski, G.; Böhmer, V.; Vogt, W. *Langmuir* **1988**, *4*, 276. (b) Ishikawa, Y.; Kunitake, T.; Matsuda, T.; Otsuka, T.; Shinkai, S. *J. Chem. Soc., Chem. Commun.* **1989**, 736. (c) Moreira, W. C.; Dutton, P. J.; Aroca, R. *Langmuir* **1995**, *11*, 3137.

(9) Shetty, A. S.; Zhang, J.; Moore, J. S. *J. Am. Chem. Soc.* **1996**, *118*, 1019.

(10) Zhang, J.; Moore, J. S. *J. Am. Chem. Soc.* **1994**, *116*, 2655.

S0002-7863(96)01549-1 CCC: $12.00

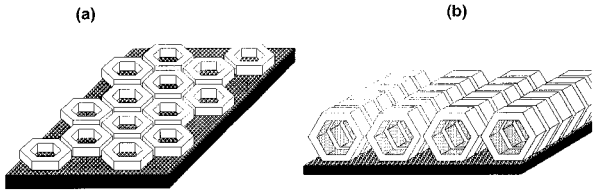

Figure 1. Limiting models of disk-shaped macrocycles at the air−water interface illustrating the effect of orientation on mean molecular area: (a) face-on orientation or (b) edge-on orientation.

Chart 1

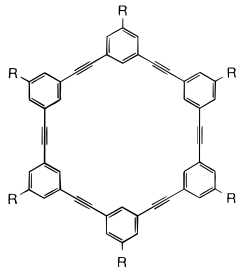

1: R = $COO^nC_4H_9$
2: R = $O^nC_6H_{13}$
3: R = $COO^tC_4H_9$
4: R = COOH
5: R = $COO^-\ N^+(^nC_4H_9)_4$
6: R = $COO^-\ N^+(CH_3)_4$

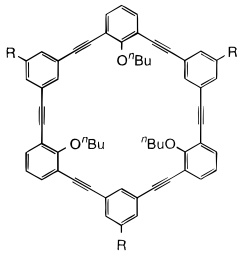

7: R = $COO^nC_4H_9$
8: R = COOH
9: R = $COO^-\ N^+(^nC_4H_9)_4$
10: R = $COO^-\ N^+(CH_3)_4$

and synthesis of a family of amphiphilic PAMs that could be induced to assemble cofacially, as monolayers, at the air−water interface and on solid surfaces. The premise is that introduction of hydrophilic pendant groups on one side of the disk-shaped PAMs can render them amphiphilic, analogous to introduction of a hydrophilic moiety at one end of a rod-like molecule. An understanding of the assembly of these amphiphilic PAMs at interfaces is crucial to the subsequent design of devices which could function as two-dimensional host matrices and shape selective membranes or sensors.

The disk-shaped amphiphilic macrocycles could, in principle, adopt either of two limiting orientations at the air−water interface depending on the spatial disposition of the functional groups appended to the phenylacetylene skeleton. PAMs could form monolayers with the plane of the macrocycle either parallel (face-on) or perpendicular (edge-on) to the interface (Figure 1).[6d] PAMs which have hydrophilic groups symmetrically arranged around the periphery of the macrocyclic skeleton should favor the face-on orientation. The chemical structures of PAMs with a hydrophilic periphery used in this study are shown in Chart 1 (**1**−**10**). The candidate macrocycles with spatially segregated hydrophobic and hydrophilic groups, such as PAMs **11**-**18** (Chart 2), were designed specifically with the premise that these molecules could be induced to form stable monolayers at the air−water interface with the edge-on orientation. Individual amphiphiles in such an orientation could pack cofacially, leading to monolayers with channels aligned parallel to the interface. On the other hand, the PAMs that adopt the face-on orientation could lead to monolayers with channels normal to the interface. This work describes the synthesis and subsequent characterization of novel amphiphilic PAMs and their fabrication into a variety of supramolecular architectures in which the assembly is directed by the underlying molecular design. In particular

(11) Venkataraman, D.; Lee, S.; Zhang, J.; Moore, J. S. *Nature*, **1994**, *371*, 591.

Chart 2

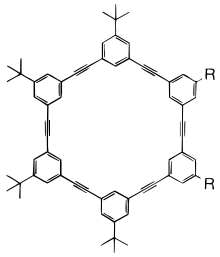

11: R = $COO^tC_4H_9$
12: R = COOH
13: R = $COO^-\ N^+(^nC_4H_9)_4$
14: R = $COO^-\ N^+(CH_3)_4$

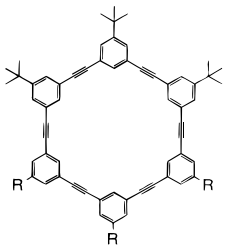

15: R = $COO^tC_4H_9$
16: R = COOH
17: R = $COO^-\ N^+(^nC_4H_9)_4$
18: R = $COO^-\ N^+(CH_3)_4$

we demonstrate that the gross orientation of the amphiphilic PAMs is predictably directed by the functionalization along the edge of the disk.

Experimental Section

General. The syntheses of PAMs **1** and **2** have been previously reported.[12] Synthetic procedures and characterization data for PAMs **3**-**18** are given in the supporting information. All compounds give satisfactory ^{1}H NMR, ^{13}C NMR, and mass analyses. Monolayers of PAM **13** were successfully transferred to substrates. The preparation procedure for PAM **13** involved conversion of the diester, PAM **11**, to the diacid, PAM **12**, by pyrolysis of the *tert*-butyl ester groups with elimination of isobutylene. This was done by heating solid diester (≈3 mg), under nitrogen, at 250 °C for 10 min. The resulting diacid was then suspended in methanol and a few drops of tetra-*n*-butylammonium hydroxide in methanol were added. After the PAM dissolved, the methanol was evaporated under a gentle stream of nitrogen. Distilled water was added to the residue and the carboxylate was extracted with chloroform.[13] NMR spectra were recorded on a Varian Unity 400. Vapor pressure osmometry (VPO) was carried out on a KNAUER vapor pressure osmometer at 308 K with benzil as the calibration standard in chloroform.

Langmuir−Blodgett Experiments. The surface pressure−area (Π−*A*) isotherms of the macrocycles were recorded at 293 K. Solvents used to prepare spreading solutions were glass-distilled HPLC grade chloroform from Baxter (stabilized with amylenes) stored under nitrogen. Monolayers were spread onto a KSV 5000 Langmuir−Blodgett system, equipped with an electronically controlled dipping device, from 6×10^{-4} to 1×10^{-3} M solutions in chloroform. The subphase was deionized and reverse osmosis purified water which was then passed through a Milli-Q Plus filtration system, yielding a final resistivity of 18.2 MΩ cm, and buffered with 10 mM sodium phosphate solutions to maintain a pH of 7.0. The buffer salts (99.9% purity) were obtained from Fisher Scientific and were used without further purification. All Π−*A* isotherms were recorded 15 min after spreading to allow solvent evaporation and/or interaction with the subphase. The barrier speed was 10 mm/min when the molecules were in the two-dimensional gas phase and changed to 1 mm/min when the surface pressure reached 1.0 mN/m. The LB monolayers were transferred to substrates at 293 K in the vertical mode (upward stroke) at a deposition rate of 10 mm/min and a surface pressure of 25 mN/m. The resultant films covered an area of approximately 1 in.^{2} on the substrate.

Monolayer Characterization. Fused silica slides were purchased from Heraeus Amersil (Duluth, GA), and *n*-doped Si(100) crystals were obtained from Von-Ruse (Caldwell, Idaho). The fused silica and Si-

(12) Zhang, J.; Pesak, D. J.; Ludwick, J. L.; Moore, J. S. *J. Am. Chem. Soc.* **1994**, *116*, 4227.

(13) Analytical data for all new compounds meet specifications and are provided in the supporting information.

(100) substrates were cleaned and rendered hydrophilic using the following treatment. Substrates were first rinsed with chloroform followed by ethyl alcohol. They were then rinsed with distilled water and dipped in boiling concentrated sulfuric acid for 10 min, followed again with rinsing in distilled water. This resulted in oxidized surfaces which were hydrophilic as determined by contact angle goniometry.

Surface wettability measurements were obtained on a custom-built contact angle goniometer, consisting of a sample platform mounted perpendicular to a rotation stage with an open circular center for illumination from the back. After application of the drop, the surface was observed using a freely rotating microscope objective (with etched crosshairs) mounted inside a calibrated goniometer. The contact angle of deionized water (Milli-Q; 18 MΩ cm) was measured on a series of 5 μL sessile (free standing) drops applied to the surface with a blunt cut syringe. Contact angles were averaged over 3−5 spots for each film.

Absorption spectra of transferred monolayers were measured on a Varian Cary-3 UV−visible spectrophotometer. Ellipsometry measurements were performed on a Gaertner Automatic Ellipsometer Model L116C at a 70° angle-of-incidence. Ellipsometry measurements were performed at 5−7 spots on each sample and averaged. The bulk refractive indices of the PAMs were obtained using a Nikon Labophot-Pol petrographic microscope and compared to Cargille Refractive Index liquids.

Transmission FT-IR spectra for N_2 dried double-sided monolayer films on SiO_2 substrates were recorded over the frequency range 3500−2500 cm^{-1} on a BioRad FTS-60A instrument equipped with a liquid-nitrogen-cooled MCT detector. This experimental configuration does not permit detection of vibrational frequencies less than 2500 cm^{-1} due to strong absorption by the bulk fused silica substrate. Spectra were recorded under N_2 at 2 cm^{-1} resolution and averaged over 256 scans to provide a high S/N ratio.

Angle-resolved XPS experiments were performed using a Physical Electronics PHI 5400 spectrometer with a Mg Kα X-ray source. The typical power of the X-ray source was approximately 400 W and the pass energy for survey scans was 179 eV, while multiplex scans were performed at 36 eV. The base pressure of the chamber was maintained below 10^{-9} Torr. The LB films deposited on substrates were mounted in the chamber and experiments performed at the equilibrium temperature of the system, which is approximately room temperature. Survey scans and C(1s), O(1s), N(1s), Si(2s), and Si(2p) levels were recorded normal to the surface as well as at 45° and 75° from the surface normal.

Results and Discussion

Behavior at the Air−Water Interface. Critical to the designed function of molecular assemblies is the orientation of the macrocycle, both at the air−water interface and after transfer to a solid substrate. Under the appropriate conditions orientational information about molecules at the air−water interface can be obtained directly from the Π−*A* isotherm.[14] The mean molecular area of the macrocycles in the solid-phase region of the isotherm is an indication of the orientation of the molecules with respect to the subphase. From the crystal structure and molecular modeling of related PAMs it is known that the macrocycle is approximately 18 Å across with *ca.* 3.5 Å between adjacent cofacially packed aromatic molecules.[10] The face of the molecule thus occupies an area of over 200 Å^2, while the edge-on orientation would be expected to give a mean molecular area of *ca.* 55 Å^2 (Figure 1). Hence, these limiting mean molecular areas can be used in conjunction with the actual isotherms to eliminate some structural models.

Surface pressure−area isotherms (Π−*A*) of PAMs **1**-**3**, **7**, **11**-**15**, and **17** are shown in Figures 2−5. PAMs **1**−**3** and **7** are appended with ester and ether groups at all six *meta* positions along their periphery (Chart 1) and, on average, showed extrapolated (to zero surface pressure) mean molecular areas (Figures 2 and 3) below 100 Å^2 ($\langle A\rangle_1 = 92 \pm 1$ Å^2/molecule, $\langle A\rangle_2 = 82 \pm 2$ Å^2/molecule, $\langle A\rangle_3 = 82 \pm 1$ Å^2/molecule, $\langle A\rangle_7 = 91 \pm 5$ Å^2/molecule). Since these values are much smaller than the 200 Å^2/molecule predicted for the face-on geometry, this indicates that these PAMs do not adopt the intended face-on orientation but must lie with the disk plane significantly out of the plane of the air−water interface. Presumably the ester

(14) See for example: Chou, H.; Chen, C.-T.; Stork, K. F.; Bohn, P. W.; Suslick, K. S. *J. Phys. Chem.* **1994**, *98*, 383.

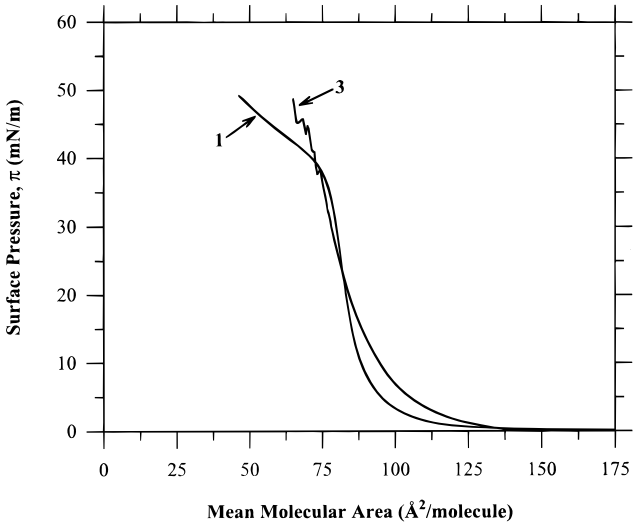

Figure 2. Π−*A* isotherm of PAMs **1** and **3** at the air−water interface (pH 7; 293 K; barrier speed = 1 mm/min).

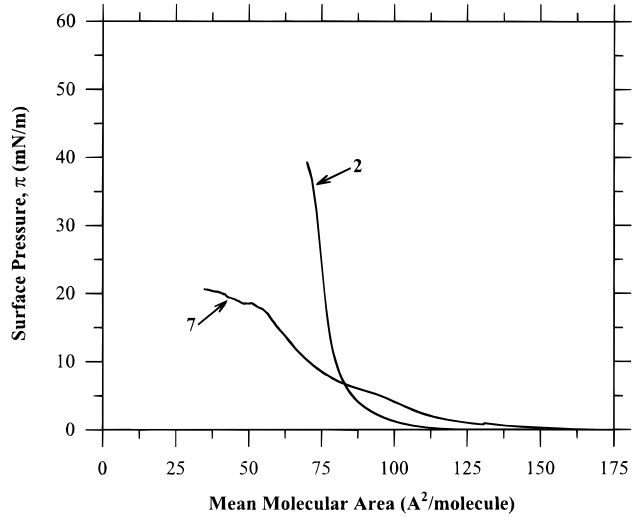

Figure 3. Π−*A* isotherm of PAMs **2** and **7** at the air−water interface (pH 7; 293 K; barrier speed = 1 mm/min).

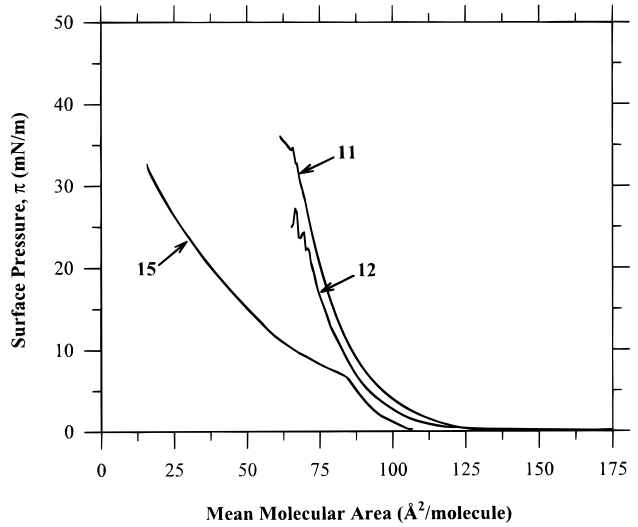

Figure 4. Π−*A* isotherm of PAMs **11**, **12**, and **15** at the air−water interface (pH 7; 293 K; barrier speed = 1 mm/min).

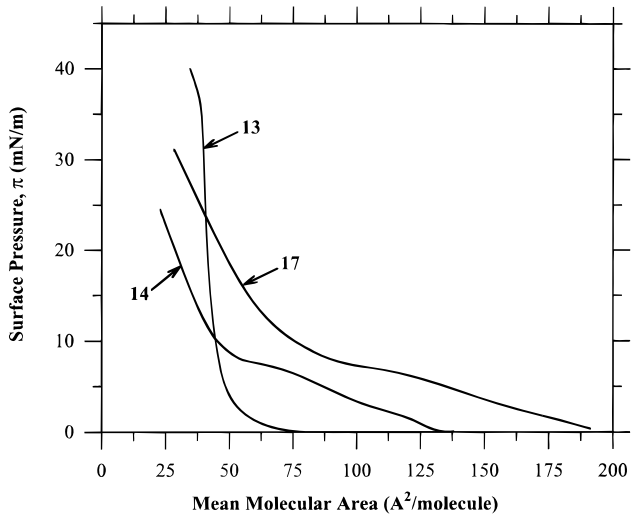

Figure 5. Π−*A* isotherm of PAMs **13**, **14**, and **17** at the air−water interface (pH 7; 293 K; barrier speed = 1 mm/min).

and ether groups are not sufficiently hydrophilic to bias the orientation of the macrocycles, although favorable macrocycle stacking interactions may also cause some slip-stacking to occur. The monolayer of PAM **7**, with three *endo*-functionalized ether groups, was particularly unstable as compared to those of PAMs **1**−**3** with *exo*-functionalized groups. The isotherm shows that the monolayer of PAM **7** collapses prior to the solid-like phase, while the monolayers of PAMs **1**−**3** exhibit well-defined solid-like regions and collapse at relatively high pressures. Therefore, changes in the positioning of the functional group in the molecular structure dramatically affect the behavior of the monolayer. PAMs **4**−**10**, functionalized with the more hydrophilic carboxylic acid or carboxylate groups along the periphery of the macrocyclic skeleton, were only soluble in solvents like THF, methanol, DMSO, DMF, and NMP, which are miscible with water and thus unsuitable for Langmuir experiments.

PAMs depicted in Chart 2 with spatially segregated hydrophobic and hydrophilic groups were designed with the premise that the positioning of the groups might induce the PAMs to adopt the edge-on orientation. PAMs **11**−**15** and **17** were all soluble in chloroform. Dilute solutions of these PAMs were deposited on the water surface in the LB trough and the Π−*A* isotherms obtained. PAMs **16** and **18** were, however, insoluble in the appropriate solvents and hence could not be deposited on the trough. The isotherms (Figure 4) show that PAMs **11** and **15** functionalized with ester groups had extrapolated mean molecular areas, $\langle A\rangle_{11} = 89 \pm 1$ Å^2/molecule and $\langle A\rangle_{15} = 83 \pm 2$ Å^2/molecule, which again favors a tilted edge-on orientation adopted by these PAMs. The monolayer of PAM **12** with the more hydrophilic carboxylic acid groups, displayed an extrapolated mean molecular area similar to those of the corresponding diester PAM **11**, although the monolayer of PAM **12** buckled at a lower pressure (20 mN/m). The less stable nature of this particular monolayer is somewhat surprising at first, but may be explained by the formation of extended intermolecular hydrogen-bonding networks. This notion is supported by variable temperature ^{1}H NMR and vapor pressure osmometry measurements of PAM **12** in various solvents (a more detailed description of these experiments is contained in the supporting information). Such hydrogen-bonded networks would require PAMs to severly deviate from the edge-on orientation, thereby reducing monolayer stability.

To disrupt hydrogen-bonded networks and to further enhance hydrophilic character, PAMs **12** and **16** were converted to the corresponding tetra-*n*-alkylammonium carboxylate salts (**13**, **14**, **17** and **18**). LB experiments were performed on the chloroform-soluble PAMs **13**, **14**, and **17** (Figure 5). Seemingly small changes in the functional groups of the PAMs affect their behavior at the air−water interface. PAMs **13** and **14** with carboxylate groups along one edge have mean molecular areas of $\langle A\rangle_{13} = 44 \pm 1$ Å^2/molecule and $\langle A\rangle_{14} = 57 \pm 1$ Å^2/molecule. On the other hand, PAM **17** with hydrophilic carboxylate groups on two edges of the macrocyclic skeleton oriented in a more tilted fashion at the air−water interface as evidenced by the extrapolated mean molecular area of $\langle A\rangle_{17} = 83 \pm 1$ Å^2/molecule. In addition, PAM **13** appended with tetra-*n*-butylammonium carboxylate salt resulted in a more robust monolayer than did PAM **14** with the tetramethylammonium salt, which exhibited an extended liquid-like phase and a lower collapse pressure. It is interesting to note that the isotherms for PAM **14**, **15**, and **17** do not show a well-defined collapse point for the monolayer, evidencing continuous behavior even at high pressures. This is most likely due to macrocycle stacking and resultant multilayer formation. Since these macrocycles initially lie flat or nearly-so at the air−water interface, increasing surface pressure may simply cause the macrocycles to slip over one another, thus preventing true monolayer formation. While this multilayer formation is interesting in and of itself, PAM **13** is unique. Its isotherm clearly exhibits a solid-like phase, which is stable over a significant increase in surface pressure and occurs at a mean molecular area consistent with a well-packed, vertically-oriented monolayer. Because PAM **13** is clearly the macrocycle system which displayed the most promising behavior for formation of robust solid films, it was chosen for further detailed study.

Transferred Films. Of all the molecules studied above, only PAM **13** could be transferred successfully from the water surface onto hydrophilic substrates, *e.g.* fused silica and Si(100). The transfers were reproducible and consistently had transfer ratios, $\tau = 1.0 \pm 0.1$. All other macrocycles exhibited poor transfer characteristics. Transferred monolayers of PAM **13** were characterized using various techniques to probe the structure of the resulting molecular assemblies.

Contact angle measurements constituted the first and simplest experiment performed to assess the transferred PAM monolayer. The surfaces which were hydrophilic prior to the transfer became hydrophobic. Before the transfer, the contact angles (θ_c) of a sessile water drop on Si(100) and fused silica were 11 ± 2° and 5 ± 2°, respectively, and after the transfer they were 63° ± 2° in both cases. This latter value is intermediate between that observed for a hydrophilic surface and typical θ_c values observed for tightly-packed (non-porous) alkane films, *e.g.* stearic acid, octadecane thiol.[1a] This suggests a structure in which a hydrophobic portion of PAM **13** is presented to the solvent, *i.e.*, carboxylates down, but in which the macrocycles are packed in such a way as to allow solvent molecules some access to the hydrophilic substrate. The closest packing distance for the macrocycles in a vertical orientation to the substrate is approximately 3.5 Å.[11] On this length scale, the water molecules can interdigitate between the macrocycle rings and access the porous (free-volume) structure of the macrocycle as well as the hydrophilic substrate. The presence of film defects can also influence the observed water contact angle. The transfer of any LB film to a substrate will inevitably be accompanied by film defects, *i.e.*, two-dimensional grain boundaries, missing molecules, and rotation faults, and to the extent that these provide ready access for water molecules to the hydrophilic SiO_2 surface, they decrease the observed contact angle. While no specific experiments have been performed herein to assess the defect density or structural characteristics of defect sites, it should be noted that a variety of real-space imaging techniques (AFM, TEM, STM) were performed to

Table 1. Comparison of Angle-Resolved XPS Intensity Ratios for a Clean Si(100) Substrate and a Monolayer of PAM **13** Transferred onto Si(100)

	relative peak areas ratios			
sample	N(1s)/ C(1s)	O(1s)/ C(1s)	Si(100 eV)/ C(1s)	Si(103 eV)/ C(1s)
bare silicon (100)				
at 0°	0.000	11.300	5.800	1.440
at 75°	0.000	4.500	0.450	0.700
monolayer of PAM **13**				
at 0°	0.013	1.550	0.800	0.250
at 75°	0.007	0.600	0.047	0.100

assess the structural characteristics inherent in these transferred films, however, the results proved to be irreproducible and therefore difficult to interpret. Thus, the contact angle measurements demonstrate that, on average, the hydrophobic surface of the PAMs is exposed which is consistent with an edge-on, or tilted edge-on, orientation.

For a more direct probe of the orientation of the macrocycle, various spectroscopic measurements were performed. The edge-on orientation of PAM **13** on the surface is also supported by angle-resolved X-ray photoelectron spectroscopy (XPS) measurements and ellipsometry. Table 1 summarizes the intensity ratios obtained in the angle-resolved XPS experiment on monolayers of PAM **13** transferred to oxidized Si(100). The survey spectrum of the blank showed three species above background, C, O, and Si. Clearly the Si and most of the O signal originates from the substrate, while the C and a fraction of the O signal originate from adventitious species adsorbed during sample handling prior to introduction to the XPS spectrometer. Significantly no N signal is seen in the blank, and the ratios of both O and Si to C decrease with increasing collection angle, consistent with a layer of carbonaceous material on the surface of the blank. Clearly N, O, and Si signals all decrease relative to the C. However, in the data for the PAM **13** monolayer the source of the C, N, and O is unambiguous; C and N signals come from the PAM, while O arises principally from the native silicon oxide. The Si, O, and N signals are ratioed to the signal for the C(1s) band, which serves in these samples as an internal standard. The PAM monolayer from **13** is composed of individual molecules each of which must have a relatively symmetric C atom abundance in depth, due to the near symmetry of the amphiphilic PAM. Since the signal ratios, X/C: X = N, O, Si, decrease in each case going from normal to 75° (from normal) collection angle, it is reasonable to conclude that the centroid of each of these elemental densities lies below the centroid for the C density in the XPS sample layer. If the C atom centroid is taken to be the midpoint of the PAM **13** monolayer, then each of the elements sampled must lie below that point. While this is exactly what is expected for O and Si, since they arise from the substrate, the signal ratio decrease for N is significant. The only source of N in these monolayers comes from the quaternary ammonium counterion, making it a unique marker. It is reasonable to assume, in the absence of a driving force for charge separation, that the cationic $N(C_4H_9)_4^+$ counterion would be paired with and reasonably close to the anionic carboxylates on each PAM. The presence of the counterion below the centroid for the C density, then, is additional supporting evidence that indeed the carboxylates are oriented down, *i.e.* toward the substrate, as would be expected if they are the hydrophobic moiety driving the assembly on the air−water and substrate interfaces.

The edge-on orientation of PAM **13** is also substantiated by ellipsometry data. For a perfectly edge-on orientation, the thickness of the monolayer would be determined by the dimensions of the constituent molecule. The crystal structure

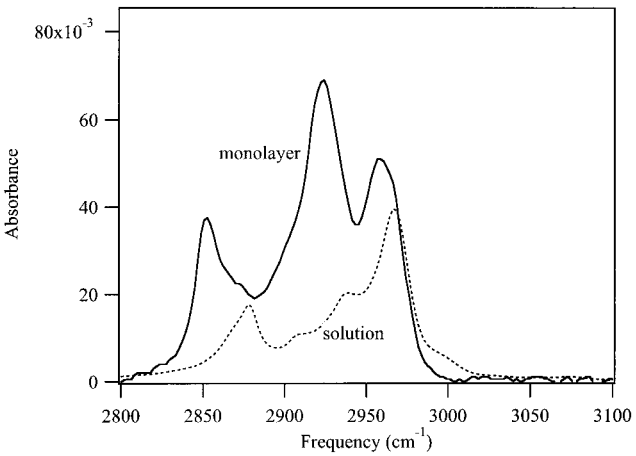

Figure 6. Infrared spectra of PAM **13**, both in $CHCl_3$ solution and at normal incidence ($\alpha = 0°$) as transferred to SiO_2 from a sodium phosphate subphase. All spectra were obtained in transmission. The spectrum for the SiO_2-supported monolayer has been background corrected to remove the residual tail of the SiO_2 absorption.

of related PAMs[11] and molecular models of the PAM **13** indicate that the ring structure of the macrocycle is approximately 18 Å in diameter. A striking correlation between the crystallographic and molecular modeling estimations of the film thickness and the actual film thickness (based on an index of refraction of 1.50 ± 0.004 determined for the bulk molecule) from the ellipsometry measurement is observed. If the index of refraction is allowed to vary from 1.4 to 1.6 (allowing for a different index of refraction of the monolayer than that of the bulk sample) in the ellipsometry data reduction procedure, the resulting film thickness changes by 3 Å. Thus, this is an appropriate estimate of the uncertainty in this experiment. The resulting film thickness for PAM **13** is 18 ± 3 Å. This degree of uncertainty precludes an exact determination that the PAMs are oriented normal to the substrate, instead a tilt angle up to 30° can be accommodated within this experimental uncertainty. Thus, the ellipsometry data establish important bounds on the orientation of PAM **13.** It is oriented within 30° of the surface normal, *i.e.*, 90° ± 30°, relative to the substrate. It is important to note that ellipsometry is a macroscopic sampling technique which results in an average film thickness over large regions of the monolayer film.

Infrared absorption spectra of PAM **13** both in solution and on the surface of fused silica (transmission geometry in both cases) are given in Figure 6. The first striking result is that the bandshapes and intensities are radically different in the transferred monolayers compared to the solution spectrum. In the monolayer spectra the absorbance at 2961 cm^{-1} has been assigned to the $\nu_{as}(CH_3)$ stretch,[15,16] while the peaks located at 2853 and 2924 cm^{-1} correspond to the symmetric, $\nu_s(CH_2)$, and asymmetric, $\nu_{as}(CH_2)$, methylene stretching modes, respectively.[14,17] The position and width of these peaks have been previously shown to be sensitive probes of two-dimensional alkyl chain packing and order in monolayer films.[15] In ordered solid or crystalline hydrocarbons with all *trans* conformation the $\nu_s(CH_2)$ and $\nu_{as}(CH_2)$ peaks are located at 2850 and 2918 cm^{-1}. In highly disordered liquid alkanes, however, the methylene stretches are blue shifted to 2856 and 2928 cm^{-1}. Since the PAM has no CH_2 moieties, CH_2 absorption can only

(15) Colthup, N. B.; Daly, L. H.; Wiberly, S. E. *Introduction to IR and Raman Spectroscopy*, 3rd ed.; Academic Press: New York, 1990, pp 216−228.

(16) Brent, S. F.; Schilling, M. L.; Marchih, L.; Wilson, W. L.; Katz, H. E.; Harris, A. L. *Chem. Mater.* **1994**, *6*, 122.

(17) LeGrange, J. D.; Markham, J. L.; Kurkjian, C. R. *Langmuir* **1993**, *9*, 1749.

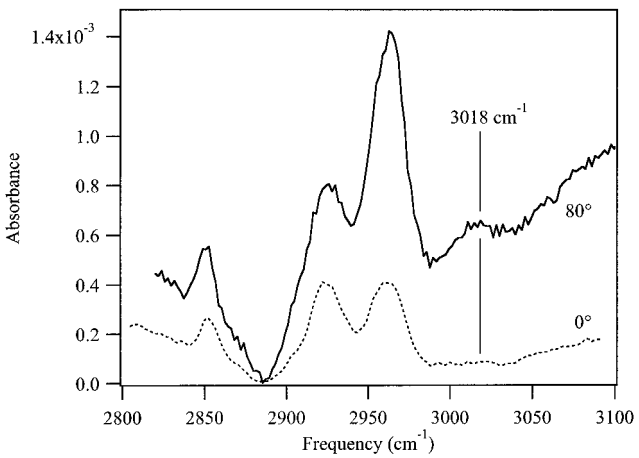

Figure 7. Polarized infrared spectra of PAM **13** as transferred to SiO_2 from a sodium phosphate subphase. Spectra were obtained with p-polarized incident radiation both at normal ($\alpha = 0°$) and grazing ($\alpha = 80°$). The spectra have been background corrected to remove the residual tail of the SiO_2 absorption.

come from the co-transferred $N(C_4H_9)_4^+$ counterion. Thus, the positions of these marker bands for ordering indicate that the $-(CH_2)-$ groups in the butyl chains are partially ordered. The solution spectrum, on the other hand, is dominated by the absorption of the methyl groups. Since there are 20 methyls and 24 methylenes in the PAM including the two counterions, and since the solution spectrum certainly is characteristic of a disordered state, the dominance of methyl absorption must result from a somewhat larger oscillator strength. This observation makes the dominance of the counterion-derived CH_2 moieties in the normal-incidence surface spectra all the more striking.

In addition Figure 7 shows that a new, albeit weak, band appears at 3018 cm^{-1}, the position expected for the aromatic in-plane ν(CH), in the spectra taken at angles of incidence $\alpha \geq 65°$. This band is very weak in all of the solution spectra, indicating its small oscillator strength relative to the aliphatic CH stretches. However, the fact that it is observed at $\alpha \geq 65°$, but not at normal incidence is significant. First, all of the aromatic C−H stretches in the PAM **13** have transition dipoles which are in the plane of the macrocycle. In addition, their azimuthal distribution within the fiducial plane of the macrocycle is symmetric. Thus, collectively they approximate a planar transition dipole, oriented in the macrocycle plane, for which,

$$\rho' = \frac{\int A_N \, d\lambda}{\int A_p \, d\lambda} = \frac{\cos \alpha}{\cos^2 \alpha + \dfrac{2 \sin^2 \alpha \sin^2 \theta}{2 - \sin^2 \theta}} \qquad (1)$$

describes the ratio of integrated absorbance at normal incidence to that obtained for p-polarized radiation at an angle-of-incidence, α.[18] The angle θ is defined to be the angle between the normal to the oscillator plane and the surface normal. Using the uncertainty in the aromatic ν(CH) band for normal incidence to define a maximum integrated absorbance yields $\rho' \geq 0.92$, for which $\theta \geq 78°$. Since this is the angle made by the macrocycle normal with the substrate normal, the orientation of the ring plane relative to the surface normal is as follows, $90° - \theta \leq 12°$. Thus, it is clear that the macrocycle plane is nearly vertically oriented. This measurement of macrocycle orientation is consistent with both the ellipsometry and XPS data discussed previously. The other readily discernible features of the spectra shown in Figure 7 are (a) the increase in absorbance at grazing angles and (b) the larger increase in the intensity of the $\nu_a(CH_3)$ stretch relative to the $\nu_a(CH_2)$ stretch at grazing incidence. However, given the fact that the CH_2 absorption is solely derived from the counterion, while the CH_3 absorption has contributions from both the PAM and the counterion, it is not possible to draw quantitative conclusions without more extensive investigations, which are currently underway.

(18) (a) Xu, Z.; Lau, S. Y.; Bohn, P. W. *Surf. Sci.* **1993**, *296*, 57. (b) Yoneyama, M.; Sugi, M.; Saito, M.; Ikegami, K.; Kuroda, S.; Iizima, S. *Jpn. J. Appl. Phys.* **1986**, *25*, 961.

Conclusions

Amphiphilic phenylacetylene macrocycles (PAMs), with molecular structures that vary in the nature and orientation of their pendant functional groups, have been studied both on a Langmuir trough and as monolayers transferred onto solid substrates. These monolayer films have potential applications as host matrices and shape selective membranes, whose two-dimensional organization should bring together shape selective compartments. The disk-like PAMs can, in principle, adopt orientations in which the plane of the molecules is either edge-on or face-on to the interface. We find that PAMs whose periphery is symmetrically hydrophilic do not prefer the face-on orientation, instead orienting in a tilted edge-on, possibly stacked, configuration. PAMs that have spatially segregated hydrophilic and hydrophobic groups adopt the edge-on orientation when they are functionalized with carboxylate groups. In contrast, PAMs appended with acid moieties give unstable monolayers, presumably because they engage in strong intermolecular hydrogen bonding interactions, as evidenced by ^1H NMR and vapor pressure osmometry of the solutions. Monolayers of the dicarboxylate PAM **13** were transferred to substrates and characterized. The characterization indicates that the macrocycles form a stable two-dimensional organization with a high degree of conformational and polar order and that they adopt the edge-on orientation, although they orient slightly tilted, *ca.* 12°, from vertical. Experiments to probe the host−guest properties of these monolayers using chromophoric guests are currently underway.

Acknowledgment. We dedicate this paper to Professor Nelson J. Leonard on the occasion of his 80th birthday. We acknowledge the contributions of Dr. Richard Haash of the Materials Research Laboratory for assistance with the XPS measurements as well as Ms. Sally E. Greenberg and Prof. Richard I. Hay in the Department of Geology for assistance with the bulk index of refraction measurements. This work was supported by the National Science Foundation through grant CHE-94−20211 and the Young Investigator Program (CHE-94−96105). Additional support from the 3M Company and the Camille Dreyfus Teacher-Scholar Awards Program (J.S.M.) is grateful acknowledged.

Supporting Information Available: Synthetic procedures, ^1H NMR, ^{13}C NMR, mass spectroscopic data, elemental analyses of PAMs **3**−**18**, and hydrogen bonding aggregation of PAM **12** (24 pages). See any current masthead page for ordering and Internet access instructions.

JA961549U